Structure and Bonding in Pentacyano(L)ferrate(II) and Pentacyano(L)ruthenate(II) Complexes (L = Pyridine, Pyrazine, and *N*-Methylpyrazinium): A Density Functional Study

Darío A. Estrin,*,† O. Yasmine Hamra,† Luca Paglieri,‡ Leonardo D. Slep,† and José A. Olabe†

Departamento de Química Inorgánica, Analítica y Química-Física and INQUIMAE, Facultad de Ciencias Exactas y Naturales, Universidad de Buenos Aires, Ciudad Universitaria-Pab II, 1428 Buenos Aires, Argentina, and Centro di Ricerca, Sviluppo e Studi Superiori in Sardegna (CRS4), P.O. Box 1048, 09100 Cagliari, Italy

Received May 16, 1996[⊗]

Density Functional Theory (DFT) at the generalized gradient approximation (GGA) level has been applied to the complexes $[Fe(CN)_5L]^{n-}$ and $[Ru(CN)_5L]^{n-}$ (L = pyridine, pyrazine, *N*-methylpyrazinium), as well as to $[Fe(CN)_5]^{3-}$ and $[Ru(CN)_5]^{3-}$. Full geometry optimizations have been performed in all cases. The geometrical parameters are in good agreement with available information for related systems. The role of the $M^{II}-L$ back-bonding was investigated by means of a L and cyanide Mulliken population analysis. For both Fe(II) and Ru(II) complexes the metal−L dissociation energies follow the ordering pyridine < pyrazine < *N*-methyl pyrazinium, consistent with the predicted σ-donating and π*-accepting abilities of the L ligands. Also, the computed metal−L bond dissociation energies are systematically smaller in the Ru(II) than in the Fe(II) complexes. This fact suggests that previous interpretations of kinetic data, showing that ruthenium complexes in aqueous solution are more inert than their iron analogues, are not related to a stronger Ru−L bond but are probably due to solvation effects.

Introduction

One of the currently investigated problems related to the electronic structure of coordination compounds is the degree of σ- and π-bonding contributions to bond strength. Although this can be approached through different experimental methods (IR, UV−visible, and NMR spectroscopy, acid−base titrations, electrochemistry, kinetics, etc.), most of them remain ambiguous in their ability to discriminate between the σ and π effects and between first- and second (solvent)-sphere interactions. Several families of compounds of the type $[MX_5L]^{n-}$ (M = Fe, Ru, Os; X = NH_3, CN^-, polypyridines, edta; L = different ligands binding through −N, −O, −S, and −P atoms) have been considered, with a focus on the M−L interactions and their relation to the thermodynamic and kinetic properties of the compound.[1−4]

The structure of transition-metal systems in the above-mentioned sense has proven to be a challenge for traditional ab initio techniques. Methods that include electron correlation effects are often required to treat these systems.[5] Since the computational cost of traditional ab-initio methods which include correlation effects increases as N^m with $m > 5$ (N is the number of basis functions of the system), the corresponding calculations are very demanding and impose serious limitations on the size of the system. An alternative approach to conventional ab initio methods is based on the use of density functional theory (DFT). DFT methodologies are very interesting from a computational point of view, since the time required in DFT methods increases as N^3, making DFT-based approaches ideally suited for large systems.

DFT has proven to be a reliable tool in the investigation of transition-metal systems.[6−7] Within DFT, the use of modern and powerful functionals,[8−10] including terms based on the electron density gradients (generalized gradient approximation), has eliminated most of the shortcomings of the simpler local functionals (Hartree−Fock−Slater and local density approximation), especially regarding the evaluation of bonding energies.[11]

In the present work we report calculated results (bond lengths and angles) for the $[Fe(CN)_5L]^{n-}$ and $[Ru(CN)_5L]^{n-}$ complexes (L = pyridine (py), pyrazine (pz), *N*-methylpyrazinium ($MePz^+$)), for which structural data are lacking in the literature. In particular, the pentacyanide−L systems have been the subject of much attention[12,13] because they are good models for systematic structural and mechanistic studies on pseudooctahedral compounds, as well as in studies of biochemical relevance.[14] Thus, the σ- and π-donor and the π-acceptor abilities of the L ligands have been analyzed, with the use of a Mulliken population analysis. Finally, the predicted trends in

* To whom correspondence should be addressed. Fax: 54-1-782-0441. E-mail: dario@q1.fcen.uba.ar.
† Universidad de Buenos Aires.
‡ CRS4.
⊗ Abstract published in *Advance ACS Abstracts,* October 1, 1996.

(1) Taube, H. *Pure Appl. Chem.* **1979**, *51*, 901.
(2) Toma, H. E.; Malin, J. M. *Inorg. Chem.* **1973**, *12*, 1039.
(3) Johnson, C. R.; Shepherd, R. E. *Inorg. Chem.* **1983**, *22*, 1117.
(4) Crutchley, B. J.; Lever, A. B. P. *Inorg. Chem.* **1982**, *21*, 2276.
(5) (a) Ehlers, A. W.; Frenking, G. *J. Am. Chem. Soc.* **1994**, *116*, 1514. (b) Krogh-Jespersen, K.; Zhang, X.; Ding, Y.; Westbrook, J. D.; Potena, J. A.; Schugar, H. J. *J. Am. Chem. Soc.* **1992**, *114*, 4345.
(6) (a) Ziegler, T. *Chem. Rev.* **1991**, *91*, 651. (b) Labanowski, J., Andzelm, J., Eds. *Theory and Applications of Density Functional Approaches to Chemistry*; Springer-Verlag: Berlin, 1990.
(7) (a) Li, J.; Schreckenbach, G.; Ziegler, T. *J. Am. Chem. Soc.* **1995**, *117*, 486. (b) Daul, C.; Baerends, E. J.; Vernooijs, P. *Inorg. Chem.* **1994**, *33*, 3538.
(8) Perdew, P. W. *Phys. Rev.* **1986**, *B33*, 8800; **1986**, *B34*, 7406 (erratum).
(9) Becke, A. D. *Phys. Rev.* **1988**, *A38*, 3098.
(10) Perdew, P. W. *Phys. Rev.* **1986**, *B33*, 8822.
(11) Becke, A. D. *J. Chem. Phys.* **1992**, *96*, 2155; **1992**, *97*, 9173.
(12) Sharpe, A. G. *The Chemistry of Cyano Complexes of the Transition Metals*; Academic Press: New York, 1976.
(13) Macartney, D. H. *Rev. Inorg. Chem.* **1988**, *9*, 101.
(14) Toma, H. E.; Batista, A.; Gray, H. B. *J. Am. Chem. Soc.* **1982**, *104*, 7509.

S0020-1669(96)00534-4 CCC: $12.00

bonding energies (M−L) are discussed in the context of the available experimental dissociation kinetics results.[15]

Computational Methodology

The calculations in this study are based on the Molecole-DFT program.[16] The Kohn−Sham self-consistent procedure is applied for obtaining the electronic density and energy through the determination of a set of one-electron orbitals.[17] Gaussian basis sets are used for the expansion of the one-electron orbitals and also for the additional auxiliary set used for expanding the electronic density. Matrix elements of the exchange-correlation potential are calculated by a numerical integration scheme.[18] The orbital and auxiliary basis sets optimized by Sim et al.[19] for DFT calculations are used for C, N, and H atoms. For Fe we used the basis set given in ref 20 and for Ru the basis set given in ref 21. The contraction patterns are (5211/411/1) for C and N, (4333/431/41) for Fe, (633321/53211/531) for Ru, and (41/1) for H. For the electronic density expansion sets the contraction patterns are (1111111/111/1) for C and N, (1111111111/111/111) for Fe, (1111111111/11111/11111) for Ru, and (111111/1) for H. A more detailed description of the technical aspects of the program is given in ref 16.

Computations are performed at the generalized gradient approximation DFT level. The correlation part is composed of the parametrization of the homogeneous electron gas given by Vosko,[22] with the gradient corrections of Perdew.[8] The expression given by Becke[9] for the gradient corrections in the exchange term has been used.

Results and Discussion

(a) $[Fe(CN)_5L]^{n-}$ (L = py, pz, $MePz^+$). We have optimized the geometries of these complexes without symmetry constraints. The results for bond lengths and angles are collected in parts A and B of Table 1, respectively. The geometries are, as expected, all close to octahedral, as shown in Figure 1. The heterocyclic ligands are planar, as are the free ligands, in all cases. The plane of the L ligand intersects at a 45° angle the equatorial plane containing the N atom of the N-heterocycle and the three C atoms of the cyanide groups, as would be predicted by stereochemical considerations. Taken as a whole, all the structures are very similar.

Experimental values of the structural parameters in these complexes are not available. However, X-ray structural data exist for $[Fe(CN)_6]^{4-}$ and $[Fe(CN)_5NO]^{2-}$, and thus the DFT performance can be assessed by comparing the measured and predicted values. For $[Fe(CN)_6]^{4-}$, the mean Fe−C distance is 1.93 Å in $K_4[Fe(CN)_6]\cdot 3D_2O$[23] and 1.91 Å in $Na_4[Fe(CN)_6]\cdot 10H_2O$,[24] while the computed DFT value is 1.976 Å. The experimental and computed C−N bond lengths are 1.17 and 1.197 Å, respectively.[23,24] Similar comparisons can be established with results for the $[Fe(CN)_5NO]^{2-}$ complex.[25,26] It is known that the crystal environment affects the experimental geometries; even for $[Fe(CN)_6]^{4-}$, the site symmetry of the metal is not perfectly octahedral, due to the anion surroundings; therefore, a perfect agreement of isolated system calculations with X-ray values is not expected. However, it appears that the DFT calculations lead to a systematic overestimation of bond distances by 0.02−0.04 Å.

The computed Fe−C bond distances are very similar for L = py, pz and are shorter for L = $MePz^+$. Also, the Fe−C1-(axial) bond length is significantly shorter than the Fe−C(equatorial) lengths for the three complexes. The strong

Table 1. Bond Distances (Å) and Angles (deg) for the $[Fe(CN)_5L]^{n-}$ Anions (L = py, pz, $MePz^+$)

	L			
	none	py	pz	$MePz^+$
	(A) Distances			
Fe−C1	1.876	1.943	1.938	1.936
Fe−C2	1.958	1.968	1.968	1.956
Fe−C3	1.961	1.967	1.968	1.957
Fe−C4	1.958	1.968	1.968	1.958
Fe−C5	1.961	1.967	1.968	1.958
Fe−N6		2.002	1.962	1.888
C1−N1	1.195	1.191	1.189	1.184
C2−N2	1.195	1.192	1.191	1.187
C3−N3	1.194	1.191	1.192	1.185
C4−N4	1.195	1.192	1.191	1.186
C5−N5	1.194	1.191	1.192	1.186
N6−C6		1.362	1.366	1.380
C6−C7		1.397	1.392	1.369
C7−N7			1.361	1.391
N7−C8			1.359	1.390
C8−C9		1.396	1.392	1.369
C9−N6		1.368	1.371	1.385
C7−C10		1.409		
C10−C8		1.408		
N7−C11				1.447
C6−H6		1.097	1.097	1.097
C7−H7		1.105	1.105	1.099
C8−H8		1.104	1.106	1.098
C9−H9		1.100	1.100	1.099
C10−H10		1.105		
C11−H10				1.117
C11−H11				1.108
C11−H12				1.108
	(B) Angles			
N6−Fe−C1		178.2	178.4	178.7
N6−Fe−C2		89.6	90.2	91.3
N6−Fe−C3		90.0	91.1	91.5
N6−Fe−C4		89.6	90.2	91.3
N6−Fe−C5		90.0	91.1	91.5
C1−Fe−C2	94.5	89.3	88.7	87.7
C1−Fe−C3	96.8	91.2	90.1	89.5
C1−Fe−C4	94.5	89.3	88.7	87.8
C1−Fe−C5	96.8	88.8	90.1	89.6
C2−Fe−C3	89.7	90.8	91.0	93.6
C2−Fe−C4	89.9	89.9	89.5	87.1
C2−Fe−C5	168.7	177.5	178.6	177.3
C3−Fe−C4	168.7	177.5	178.6	177.2
C3−Fe−C5	88.4	88.6	88.5	86.1
C4−Fe−C5	89.7	90.8	91.0	93.1
Fe−N6−C6		119.7	121.1	121.1
Fe−N6−C9		152.5	125.1	124.0
C9−N6−C6		116.3	113.8	114.8
N6−C6−C7		123.3	122.3	123.1
N6−C9−C8		123.5	122.4	123.3
C6−C7−N7			124.6	121.4
C9−C8−N7			124.4	121.0
C8−N7−C7			112.3	116.2
C6−C7−C10		120.3		
C9−C8−C10		120.0		
C8−C10−C7		116.5		
N7−C11−H10				112.6
N7−C11−H11				109.6
N7−C11−H12				109.7

(15) Hoddenbagh, J. M. A.; Macartney, D. H. *Inorg. Chem.* **1986**, *25*, 9173.
(16) Estrin, D. A.; Corongiu, G.; Clementi, E. In *METECC, Methods and Techniques in Computational Chemistry*, Clementi, E., Ed.; Stef: Cagliari, Italy, 1993; Chapter 12.
(17) Kohn, W.; Sham, L. J. *Phys. Rev.* **1965**, *A140*, 1133.
(18) Becke, A. D. *J. Chem. Phys.* **1988**, *88*, 1053.
(19) (a) Sim, F.; Salahub, D. R.; Chin, S.; Dupuis, M. *J. Chem. Phys.* **1991**, *95*, 4317. (b) Sim, F.; St-Amant, A.; Papai, I.; Salahub, D. R. *J. Am. Chem. Soc.* **1992**, *114*, 4391.
(20) Andzelm, J.; Radzio, E.; Salahub, D. R. *J. Comput. Chem.* **1985**, *6*, 520.
(21) Basis set obtained from the World Wide Web: http://www.cray.com/PUBLIC/APPS/UNICHEM/whatsnew.html.
(22) Vosko, S. H.; Wilk, L.; Nusair, M. *Can. J. Phys.* **1980**, *58*, 1200.
(23) Taylor, J. C.; Mueller, M. H.; Hitterman, R. L. *Acta Crystallogr.* **1974**, *A26*, 559.
(24) Tullberg, A.; Vannerberg, N. G. *Acta Chem. Scand.* **1974**, *A28*, 551.
(25) Bottomley, F.; White, P. S. *Acta Crystallogr.* **1979**, *B35*, 2193.
(26) Estrin, D. A.; Baraldo, L. M.; Slep, L. D.; Barja, B. C.; Olabe, J. A.; Paglieri, L.; Corongiu, G. *Inorg. Chem.* **1996**, *35*, 3897.

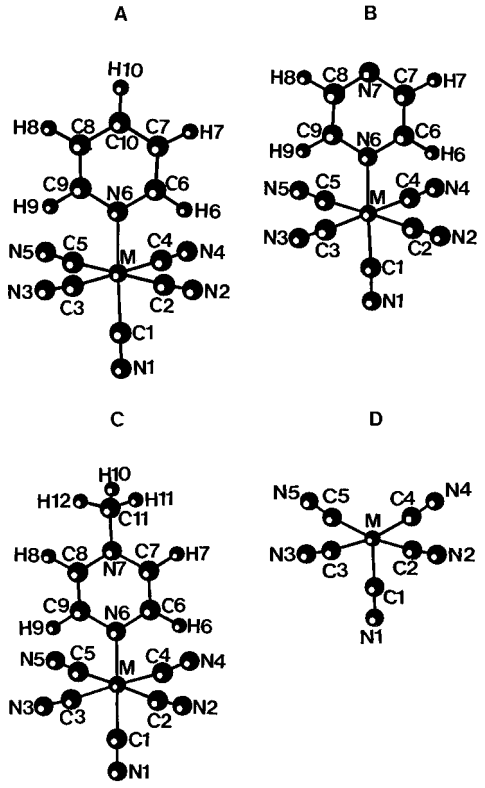

Figure 1. Structure of $[M(CN)_5L]^{n-}$ ions in vacuo: (A) L = py; (B) L = pz, (C) L = $MePz^+$, (D) pentacyano derivative (M = Fe, Ru).

electron-withdrawing ability of $MePz^+$ induces a greater depletion of the population of σ- and π-donor and π^*-acceptor cyanide orbitals for the $MePz^+$ derivative, compared to the pyridine and pyrazine derivatives (Table 2); this makes the Fe−C bonds shorter for the $MePz^+$ complex, particularly that trans to the $MePz^+$ ligand. The changes in donor and acceptor orbital populations go in opposite senses if the influence on the Fe−C distance is considered; we conclude that σ- and π-donor effects predominate over π^*-acceptor effects.

The Fe−N(L) bond distances follow the ordering: 2.002 Å (py) > 1.962 Å (pz) > 1.888 Å ($MePz^+$)). The trends correlate well with the σ and π^* populations of the L ligand (Table 2); as one goes to the right, the back-bonding increases because of the lower energy of the LUMO (π^*); thus, the orbital population of π^* also increases and the M−N bond becomes shorter. Through a synergistic effect $MePz^+$ also becomes a moderately strong σ-donor, as shown by the population changes of the σ-donor orbitals, thus reinforcing the shortening of the M−N bond.

The C−N bond distances are shorter in the $MePz^+$ complex than in the py and pz species. This is ascribed to the smaller population in the cyanide π^* antibonding orbitals in the $MePz^+$ case, due to the fact that the positive ligand competes most favorably with the cyanides for the π-electron density. For the $[Fe(CN)_5NO]^{2-}$ ion, the calculated C−N bond lengths were even shorter (around 1.182 Å), consistent with the very strong electron-acceptor ability of nitrosyl.[26]

We have also performed a geometry optimization of the $[Fe(CN)_5]^{3-}$ system. The singlet species has been found to be the most stable. The results are collected in Table 1. The optimized geometry can be regarded as having a distorted-octahedral structure in which one of the axial sites is vacant. The equatorial Fe−C bond lengths are shorter than in the pyridine and pyrazine derivatives and are similar to those in the $MePz^+$ complex. The shortening of the Fe−C bond is particularly significant for the axial atoms. When going to the right in Table 1A, we predict a decrease in back-bonding to π^*(CN), thus lengthening the Fe−C bond; on the other hand, we expect an increase in σ donation from cyanides to the metal, which should act in the opposite sense. It is probable that for the pentacyanide species the stronger π interaction is dominant, thus explaining the shorter Fe−C bonds; this is consistent with the corresponding increase in C−N bond length, associated with the greater population of π^* orbitals (cf. Table 2). The similar values of Fe−C bond lengths for the pentacyanide and L = $MePz^+$ species can be related to the compensation of σ-donor and π^*-acceptor influences on the Fe−C interaction.

Table 2. Cyanide and L Orbital Populations and Atomic Mulliken Populations in $[Fe(CN)_5]^{3-}$ and $[Fe(CN)_5L]^{n-}$ (L = py, pz, $MePz^+$)[a]

	L			
	none	py	pz	$MePz^+$
A. Orbital Populations				
σ'(L)		2.00	1.927	1.976
π(L)		1.978	1.985	1.982
σ(L)		1.765	1.820	1.732
π^*(L)		0.314	0.409	0.911
$\sigma(CN)_{eq}$	1.324	1.289	1.274	1.229
$\pi(CN)_{eq}$	3.978	3.968	3.964	3.940
$\pi^*(CN)_{eq}$	0.024	0.03	0.010	0.00
$\pi'^*(CN)_{eq}$	0.125	0.115	0.105	0.088
$\sigma(CN)_{eq}$	1.272	1.285	1.288	1.265
$\pi(CN)_{eq'}$	3.971	3.979	3.982	3.953
$\pi^*(CN)_{eq'}$	0.015	0.02	0.01	0.00
$\pi'^*(CN)_{eq'}$	0.123	0.111	0.101	0.063
$\sigma(CN)_{ax}$	1.273	1.282	1.276	1.244
$\pi(CN)_{ax}$	3.987	3.968	3.948	3.928
$\pi^*(CN)_{ax}$	0.084	0.110	0.207	0.186
$\pi'^*(CN)_{ax}$	0.156	0.100	0.093	0.073
B. Atomic Mulliken Populations[b]				
Fe	−0.6487	−0.7666	−0.7670	−0.7821
C1	0.0144	−0.0233	−0.1076	−0.1089
N1	−0.5122	−0.4851	−0.4620	−0.3508
C2	−0.0226	0.1064	0.1394	0.1570
N2	−0.4898	−0.5054	−0.4996	−0.4033
C3	0.0914	0.1274	0.1008	0.1056
N3	−0.5057	−0.5155	−0.5034	−0.4107
C4	−0.0226	0.1064	0.1394	0.1566
N4	−0.4898	−0.5054	−0.4996	−0.4017
C5	0.0914	0.1274	0.1008	0.1120
N5	−0.5057	−0.5055	−0.5034	−0.4098
N6		−0.0721	−0.2086	−0.2580
C6		0.3573	0.3381	0.3260
C7		−0.0298	0.0422	0.0694
C8		−0.1155	0.0494	0.0645
C9		0.1384	0.2451	0.2408
N7			−0.3173	−0.2323
C10		0.0375		
C11				0.1907
H6		−0.0263	−0.0468	−0.0078
H7		−0.1387	−0.1113	−0.0481
H8		−0.1414	−0.1140	−0.0538
H9		0.0057	−0.0145	0.0114
H10		−0.1659		0.0296
H11				0.0034
H12				0.0001

[a] σ'(L) = σ(L) orbital of lower energy; π'^*(CN) = higher energy π^*(CN) orbitals (11th, 12th and 14th, 15th MO). [b] The entries are net charges on the atoms.

(b) $[Ru(CN)_5L]^{n-}$ (L = py, pz, $MePz^+$). The geometries of these complexes have been optimized without symmetry constraints. The results for bond distances and angles are collected in parts A and B of Table 3, respectively. As in the Fe(II) species, the geometries of the complexes are very close to octahedral (Figure 1) and show the same characteristics regarding the heterocyclic ligand plane as in the Fe(II) systems.

There are no available experimental values for Ru−C bond lengths in the pentacyano−N-heterocyclic complexes, but values

Table 3. Bond Distances (Å) and Angles (deg) for the $[Ru(CN)_5L]^{n-}$ Anions (L = py, pz, $MePz^+$)

	L			
	none	py	pz	$Mepz^+$
	A. Distances			
Ru−C1	1.957	2.053	2.060	2.065
Ru−C2	2.139	2.138	2.141	2.129
Ru−C3	2.135	2.135	2.135	2.128
Ru−C4	2.139	2.138	2.141	2.130
Ru−C5	2.135	2.135	2.135	2.127
Ru−N6		2.238	2.174	2.076
C1−N1	1.194	1.190	1.189	1.185
C2−N2	1.192	1.192	1.190	1.186
C3−N3	1.192	1.190	1.189	1.185
C4−N4	1.192	1.192	1.190	1.186
C5−N5	1.192	1.190	1.189	1.185
N6−C6		1.357	1.361	1.375
C6−C7		1.400	1.396	1.371
C7−N7			1.358	1.389
N7−C8			1.357	1.389
C8−C9		1.399	1.394	1.370
C9−N6		1.361	1.365	1.380
C7−C10		1.407		
C10−C8		1.407		
N7−C11				1.450
C6−H6		1.099	1.098	1.097
C7−H7		1.105	1.107	1.099
C8−H8		1.104	1.106	1.098
C9−H9		1.102	1.103	1.100
C10−H10		1.106		
C11−H10				1.116
C11−H11				1.108
C11−H12				1.109
	B. Angles			
N6−Ru−C1		178.6	178.7	179.2
N6−Ru−C2		88.1	88.6	89.6
N6−Ru−C3		88.5	89.2	89.5
N6−Ru−C4		88.1	88.6	89.3
N6−Ru−C5		88.5	89.2	89.3
C1−Ru−C2	93.4	90.9	90.5	90.1
C1−Ru−C3	95.7	92.6	91.8	91.2
C1−Ru−C4	93.4	90.9	90.5	90.0
C1−Ru−C5	95.7	92.6	91.8	91.1
C2−Ru−C3	89.5	90.5	90.9	93.0
C2−Ru−C4	91.0	90.1	89.8	87.3
C2−Ru−C5	170.8	176.5	177.6	178.9
C3−Ru−C4	170.8	176.5	177.6	178.8
C3−Ru−C5	88.7	88.7	88.3	86.9
C4−Ru−C5	89.5	90.5	90.9	92.7
Ru−N6−C6		119.4	120.7	121.0
Ru−N6−C9		122.9	124.3	123.1
C9−N6−C6		117.7	115.0	115.9
N6−C6−C7		122.6	121.7	122.5
N6−C9−C8		122.9	121.9	122.8
C6−C7−N7			124.2	121.1
C9−C8−N7			123.9	120.7
C8−N7−C7			113.2	116.8
C6−C7−C10		119.9		
C9−C8−C10		119.6		
C8−C10−C7		117.3		
N7−C11−H10				112.3
N7−C11−H11				109.5
N7−C11−H12				109.7

of 2.02 and 2.05 Å have been reported for $Na_4[Ru(CN)_6]\cdot 10H_2O$[27] and for $Na_2[Ru(CN)_5NO]\cdot 2H_2O$,[28] respectively. The results in Table 3A and our calculated value for the $Ru(CN)_6^{4-}$ anion, 2.147 Å, agree with expectations (within the above-mentioned systematic difference). The trends in the Ru−C bond lengths for the three $[Ru(CN)_5L]^{n-}$ complexes are the same as

Table 4. Cyanide and L Orbital Populations and Atomic Mulliken Populations in $[Ru(CN)_5]^{3-}$ and $[Ru(CN)_5L]^{n-}$ (L = py, pz, $Mepz^+$)[a]

	L			
	none	py	pz	$Mepz^+$
	A. Orbital Populations			
σ'(L)		2.00	1.965	1.986
π(L)		1.981	1.986	1.984
σ(L)		1.839	1.854	1.796
π*(L)		0.234	0.333	0.867
$\sigma(CN)_{eq}$	1.455	1.434	1.430	1.411
$\pi(CN)_{eq}$	3.988	3.970	3.967	3.940
$\pi^*(CN)_{eq}$	0.012	0.00	0.000	0.00
$\pi'^*(CN)_{eq}$	0.127	0.129	0.122	0.104
$\sigma(CN)_{eq}$	1.402	1.407	1.413	1.416
$\pi(CN)_{eq'}$	3.980	3.974	3.974	3.940
$\pi^*(CN)_{eq'}$	0.00	0.00	0.00	0.00
$\pi'^*(CN)_{eq'}$	0.130	0.129	0.119	0.091
$\sigma(CN)_{ax}$	1.245	1.395	1.401	1.398
$\pi(CN)_{ax}$	3.990	3.972	3.950	3.915
$\pi^*(CN)_{ax}$	0.071	0.142	0.177	0.185
$\pi'^*(CN)_{ax}$	0.217	0.138	0.126	0.098
	B. Atomic Mulliken Populations[b]			
Ru	0.5109	0.6942	0.7519	0.9062
C1	−0.1629	−0.3404	−0.3564	−0.4189
N1	−0.5050	−0.4858	−0.4702	−0.3463
C2	−0.2609	−0.1902	−0.1708	−0.1794
N2	−0.4987	−0.5207	−0.5108	−0.4172
C3	−0.1496	−0.1050	−0.1390	−0.1533
N3	−0.5124	−0.5372	−0.5243	−0.4323
C4	−0.2609	−0.1902	−0.1708	−0.1792
N4	−0.4986	−0.5208	−0.5108	−0.4176
C5	−0.1496	−0.1049	−0.1390	−0.1525
N5	−0.5124	−0.5371	−0.5243	−0.4320
N6		−0.1924	−0.2636	−0.2822
C6		0.3027	0.3151	0.2652
C7		0.0241	0.0437	0.0894
C8		−0.0482	0.0373	0.0714
C9		0.1509	0.1992	0.1576
N7			−0.3041	−0.2304
C10		0.0419		
C11				0.1888
H6		−0.0236	−0.0412	−0.0075
H7		−0.1300	−0.1010	−0.0435
H8		−0.1333	−0.1038	−0.0488
H9		0.0025	−0.0171	0.0171
H10		−0.1566		0.0358
H11				0.0064
H12				0.0031

[a] σ'(L) = σ(L) orbital of lower energy; π'^*(CN) = higher energy π^*(CN) orbitals (11th, 12th and 14th, 15th MO). [b] The entries are net charges on the atoms.

for the Fe(II) complexes and are also consistent with the Mulliken population analysis presented in Table 4, which was analyzed above. The computed C−N bond lengths (Table 3A) are again in consistent agreement with the value for $Ru(CN)_6^{4-}$ (1.195 Å) and compare well with experimental data for the above-mentioned salts (ca. 1.15−1.16 Å). The errors for the ruthenium complexes are larger than for the Fe(II) complexes, and this is probably due to the neglect of relativistic effects, which are known to contract the metal−ligand bond distances.[7]

The computed Ru−N(L) bond distances decrease in the order 2.238 Å (py) > 2.174 Å (pz) > 2.076 Å ($MePz^+$). The same trend was found for the measured values in the related $[Ru(NH_3)_5L]^{n+}$ series: 2.006 Å (pz)[29] > 1.95 Å ($MePz^+$).[30] The variation of the Ru−N bond lengths has been discussed in terms of the degree of the Ru−N back-bonding interaction. This is supported by calculated bond lengths in Table 3A, as well as

(27) Gentil, L. A.; Navaza, A.; Olabe, J. A.; Rigotti, G. E. *Inorg. Chim. Acta* **1991**, *179*, 89.
(28) Olabe, J. A.; Gentil, L. A.; Rigotti, G. E.; Navaza, A. *Inorg. Chem.* **1984**, *23*, 4297.
(29) Gress, M. E.; Creutz, C.; Quicksall, C. O. *Inorg. Chem.* **1981**, *20*, 1522.
(30) Wishart, J. F.; Bino, A.; Taube, H. *Inorg. Chem.* **1986**, *25*, 3318.

Table 5. Bond Dissociation Energies (kcal/mol) for $[Fe(CN)_5L]^{n-}$ and $[Ru(CN)_5\ L]^{n-}$ (L = py, pz, $MePz^+$)

	py	pz	$Mepz^+$
Fe	17.8	30.3	237.3
Ru	8.3	19.7	218.7

by the calculated Mulliken populations (Table 4), which show trends similar to those previously discussed for the iron complexes (Table 2).

In the $[Ru(CN)_5]^{3-}$ species, the same arguments as for the Fe(II) complexes hold; however, since the degree of back-bonding from the Ru(II) to the π^*(L) orbital is smaller, the effects are less pronounced. Thus, the Ru−C equatorial bond lengths are practically the same in the $[Ru(CN)_5L]^{3-}$ (L = py and pz) and in the intermediate $[Ru(CN)_5]^{3-}$ and slightly longer than in $[Ru(CN)_5\ MePz]^{2-}$. With regard to the Ru−C axial bond, the shortening after removal of the L ligand is even more pronounced than in the Fe(II) case. The small increase in the C−N bonds, compared with that in the pentacyano−L complexes, is consistent with the increase in cyanide π^* antibonding orbital populations.

(c) L Bond Dissociation Energies. We have performed calculations of the bond dissociation energies of the N-heterocyclic ligands, which correspond to the reaction enthalpy of the process

$$[M(CN)_5L]^{(3-n)-} \rightarrow [M(CN)_5]^{3-} + L^{n+} \qquad (1)$$

Only the electronic contribution to this enthalpy has been computed, neglecting zero-point energies and thermal corrections. It is important also to point out that the computed bond energies correspond to a hypothetical situation, in which there are no interactions with the medium. This point will be discussed in more detail below. The results are collected in Table 5. For both Fe(II) and Ru(II) species the bond dissociation energies follow the trend py < pz < $MePz^+$. This is consistent with the trends in the Mulliken populations of the L ligands, especially with the increase in back-bonding on going to a stronger acceptor ligand.

The ligand substitution reactions of the pentacyanoferrate-(II) and pentacyanoruthenate(II) complexes

$$[M(CN)_5L]^{(3-n)-} + L'^{m+} \rightarrow [M(CN)_5L']^{(3-m)-} + L^{n+} \qquad (2)$$

have been the subject of many mechanistic investigations.[15,31,32] Experimental information is consistent with a dissociative mechanism for ligand substitution in these complexes. This means that ligand substitution involves the formation of an intermediate and is controlled by the nature of the leaving group L^{n+}. In the Fe(II) case, it has been postulated that the intermediate is $[Fe(CN)_5]^{3-}$.[31] The activation enthalpies in aqueous solution have been found to be 24.8, 26.4, and 27.5 kcal/mol for py, pz, and $MePz^+$ Fe(II) complexes[33] and 25.6, 22.4, and 24.5 kcal/mol for py, pz, and $MePz^+$ Ru(II) complexes, respectively.[15]

DFT predicted values for bond dissociation energies in organometallics are in good agreement with the experimental results in the gas phase.[34] It is not trivial, however, to obtain, from the experimental activation enthalpies in aqueous solution, information about the intrinsic bond dissociation energies, since both the latter together with solvation effects determine the observed values.

It is known that solvation effects are essential in the understanding of the properties, reactivity, and spectroscopy of many related complexes in solution.[26,35] In this case, it can be noted that the experimental activation energies are very similar for the three studied ligands, in contrast with the computed intrinsic bond energies. Particularly, for both Fe(II) and Ru(II) complexes, the computed values obtained for the $MePz^+$ ligand are much larger than those obtained for py and pz. This fact can be easily explained in terms of the larger solvent dielectric stabilization of the charged products ($[M(CN)_5]^{3-}$ and $MePz^+$) in the $MePz^+$ case, compared to the py and pz cases.

It also follows from Table 5 that the computed bond dissociation energies for Ru(II) complexes are smaller than for Fe(II) complexes. However, the Ru complexes are more inert than the Fe species with respect to substitution of the L ligand.[13] This decreased lability has been explained in terms of a relatively stronger Ru−L bond, related to a larger degree of back-donation to the L ligand, allowed by the larger extension of the 4d Ru orbitals.[13] This has been put into question by some NMR and basicity studies on the bound L ligands, which suggest that the back-bonding to L is stronger in Fe than in Ru for the $[M(CN)_5L]^{n-}$ complexes. It has been found, for instance, that bound pz is more basic for the Fe(II) than for the Ru(II) complex.[36] Our results of the Mulliken population analysis (Tables 2 and 4) also suggest that the back-bonding is stronger in the iron systems. Besides, σ bonding strength should also be taken into account for the interpretation of dissociation bond energies.

In metal-carbonyl bond dissociation theoretical studies[7] it has been found that Fe−CO bonds are stronger than Ru−CO bonds, and the same has been found on comparing other 3d and 4d metals, such as Ni, Pd and Cr, Mo. The available experimental results in the gas phase confirm these observations.[7]

An explanation for the kinetic dissociation results should be related to solvation effects. Since a quantitative treatment of solvent effects requires the determination of the free energy or potential of mean force of the dissociation reaction in solution, which is beyond the scope of this work, we will give only a qualitative discussion.

In the iron species the back-donation to the N-heterocyclic ligand is more important than in the Ru case; thus, in the pentacyano intermediate, a larger π electron density available after dissociation shifts into the cyanides, which bear a larger negative charge. The net total charges on the cyanides, obtained from a Mulliken population analysis (Table 2B), are −2.36 in the intermediate and −2.07, −2.07, and −1.56 in the py, pz, and $MePz^+$ complexes, respectively. This results in a more favorable solvation of the intermediate with respect to the pentacyano−L complexes. Therefore, the activation enthalpy in water is expected to be smaller than the computed predicted bond dissociation energy in vacuo.

For the Ru species, the back-donation to the L ligand is smaller. The total net charge on the cyanides (Table 4B) in this case is −3.50 in the intermediate and −3.55, −3.51, and −3.12 in the py, pz, and $MePz^+$ complexes, respectively. The solvation of the intermediate in this case is not so favorable with respect to the pentacyano−L complexes as in the iron species. Therefore, the solvent is not expected to affect the activation enthalpies as much as in the iron case.

(31) Stochel, G.; Chatlas, J.; Martinez, P.; van Eldik, R. *Inorg. Chem.* **1992**, *31*, 5480.
(32) Burgess, J.; Patel, M. S. *J. Chem. Soc., Faraday Trans.* **1993**, *89*, 783.
(33) Toma, H. E.; Malin, J. M. *Inorg. Chem.* **1973**, *12*, 1039.
(34) Li, J.; Schreckenbach, G.; Ziegler, T. *J. Phys. Chem.* **1994**, *98*, 4838.
(35) Stravrev, K. K.; Zerner, M. C.; Meer, T. J. *J. Am. Chem. Soc.* **1995**, *117*, 8684.
(36) Parise, A. R.; Pollak, S.; Slep, L. D.; Olabe, J. A. *An. Asoc. Quim. Argent.* **1995**, *83*, 211.

Since the differences in bond dissociation energies between Fe(II) and Ru(II) complexes are small (about 10 kcal/mol) and are of the same order of magnitude as H-bond interaction energies, solvent effects become crucial in determining the reactivity of these systems.

Conclusions

We have shown that DFT-based techniques at the GGA level can provide a useful tool in studies of the structure and dissociation reactivity of $[Fe(CN)_5L]^{n-}$ and $[Ru(CN)_5L]^{n-}$ complexes. The structural parameters obtained are consistent with the results of a Mulliken population analysis performed for the cyanide and L orbitals. Even if the methodology shows some systematic deficiencies in the prediction of structural parameters, compared to experimental results, the computed trends are correct and useful in the understanding of the properties of these systems.

A comment is in order in reference to the M−L back-bonding computed in the $[M(CN)_5L]^{n-}$ species, as shown by the Mulliken populations. By comparison with preliminary calculations performed on the $[Ru(NH_3)_5pz]^{2+}$ species, it can be seen that the back-bonding is stronger in the $[Ru(CN)_5pz]^{3-}$ ion (π^* population 0.333) than in the pentaammine ion (π^* population 0.076). This disagrees with the usual interpretation of p*K* experimental results in the literature, which states that the $Ru(CN)_5^{3-}$ moiety is a weaker π donor than $Ru(NH_3)_5^{2+}$, due to the π-acceptor ability of the cyanides and the lack of this capability for NH_3.[37] It should be pointed out that these explanations correspond to aqueous solution experimental results, for which there is no simple way to factor out the effects of the solvent on the apparent back-bonding trends. An empirical approach for dealing with specific solute−solvent interactions has been given by Gutmann.[38] Relative donor (*DN*) and acceptor (*AN*) numbers are defined to describe the solvent's Lewis base and acid character, respectively. Solvents acting as acceptors help in stabilizing negative charge on ligands, thus increasing the back-bonding in π-acceptor ligands. On the other hand, donor solvents stabilize positive charge on ligands. The role of the solvent in the above-mentioned experimental results can be understood in terms of the donor and acceptor behavior of water in the ammine and cyanide complexes, respectively. We have shown recently the importance of these second-sphere interactions for the $[Fe(CN)_5NO]^{2-}$ ion.[26] It has also been shown that the chemistry of $[M(CN)_5L]^{n-}$ systems changes greatly on going from water to organic solutions.[39]

For the three ligands considered, the bond dissociation energy in vacuo has been found to be larger for the Fe(II) than for the Ru(II) complexes. This result also disagrees with observations in the literature, which do not take into account solvent effects.

It has been shown that DFT calculations for the isolated ions provide useful information regarding structure and bonding in these systems. However, it is extremely important to discern between intrinsic (or first sphere) and solvent (or outer sphere) effects. The latter seem to be essential in the understanding of the behavior of pentacyano(L)iron(II) and ruthenium(II) complexes.

Further calculations using different schemes for treating solvent effects within the DFT methodology, such as the continuum reaction-field approach[40] and coupled potential models,[41] are in progress in our laboratory.

Acknowledgment. This investigation was partially supported by the "Regione Autonoma della Sardegna" and by the University of Buenos Aires. D.A.E. and O.Y.H. acknowledge the Fundación Antorchas (Argentina) for financial support. D.A.E. and J.A.O. are members of the scientific staff of CONICET (National Scientific Council of Argentina).

IC960534U

(37) Johnson, C. R.; Shepherd, R. E. *Inorg. Chem.* **1983**, *22*, 2439.
(38) Gutmann, V. *The Donor-Acceptor Approach to Molecular Interactions*; Plenum: New York, 1980; *Electrochimica Acta* **1976**, *21*, 661.
(39) (a) Toma, H. E.; Takasugi, M. S. *J. Solution Chem.* **1983**, *12*, 547. (b) Toma, H. E.; Takasugi, M. S. *J. Solution Chem.* **1989**, *18*, 575.
(40) Paglieri, L.; Corongiu, G.; Estrin, D. A. *Int. J. Quantum. Chem.* **1995**, *56*, 615.
(41) (a) Field, M. J.; Bash, P. A.; Karplus, M. *J. Comput. Chem.* **1990**, *11*, 700. (b) Estrin, D. A.; Liu, L.; Singer, S. J. *J. Phys. Chem.* **1992**, *96*, 5325.